# Ocean (de)oxygenation from the Last Glacial Maximum to the twenty-first century: insights from Earth System models

L. Bopp, L. Resplandy, A. Untersee, P. Le Mezo, M. Kageyama

PHILOSOPHICAL TRANSACTIONS A

rsta.royalsocietypublishing.org

Research

**Cite this article:** Bopp L, Resplandy L, Untersee A, Le Mezo P, Kageyama M. 2017 Ocean (de)oxygenation from the Last Glacial Maximum to the twenty-first century: insights from Earth System models. *Phil. Trans. R. Soc. A* **375**: 20160323.
http://dx.doi.org/10.1098/rsta.2016.0323

Accepted: 27 March 2017

One contribution of 11 to a discussion meeting issue 'Ocean ventilation and deoxygenation in a warming world'.

**Subject Areas:**
oceanography, biogeochemistry

**Keywords:**
ocean deoxygenation, Last Glacial Maximum and future projections, Earth System modelling

**Author for correspondence:**
L. Bopp
e-mail: bopp@lmd.ens.fr

Electronic supplementary material is available online at https://dx.doi.org/10.6084/m9.figshare.c.3816625.

THE ROYAL SOCIETY PUBLISHING



# Ocean (de)oxygenation from the Last Glacial Maximum to the twenty-first century: insights from Earth System models

L. Bopp[1,2], L. Resplandy[3], A. Untersee[2], P. Le Mezo[4] and M. Kageyama[4]

[1]LMD/IPSL, CNRS/ENS/Ecole Polytechnique/UPMC, Paris, France
[2]Ecole Normale Supérieure, Département de Géosciences, Paris, France
[3]Princeton University, Geosciences Department, Princeton Environmental Institute, Princeton, NJ, USA
[4]LSCE/IPSL, CNRS/CEA/ UVSQ, CE Saclay, Gif sur Yvette, France

LB, 0000-0003-4732-4953

All Earth System models project a consistent decrease in the oxygen content of oceans for the coming decades because of ocean warming, reduced ventilation and increased stratification. But large uncertainties for these future projections of ocean deoxygenation remain for the subsurface tropical oceans where the major oxygen minimum zones are located. Here, we combine global warming projections, model-based estimates of natural short-term variability, as well as data and model estimates of the Last Glacial Maximum (LGM) ocean oxygenation to gain some insights into the major mechanisms of oxygenation changes across these different time scales. We show that the primary uncertainty on future ocean deoxygenation in the subsurface tropical oceans is in fact controlled by a robust compensation between decreasing oxygen saturation ($O_{2sat}$) due to warming and decreasing apparent oxygen utilization (AOU) due to increased ventilation of the corresponding water masses. Modelled short-term natural variability in subsurface oxygen levels also reveals a compensation between $O_{2sat}$ and AOU, controlled by the latter. Finally, using a model simulation of the LGM, reproducing data-based reconstructions of past ocean (de)oxygenation, we show that the deoxygenation trend of the subsurface

ocean during deglaciation was controlled by a combination of warming-induced decreasing $O_{2sat}$ and increasing AOU driven by a reduced ventilation of tropical subsurface waters.

This article is part of the themed issue 'Ocean ventilation and deoxygenation in a warming world'.

## 1. Introduction

Oxygen is a fundamental resource for aerobic life in oceans, and, as such, any diminution in oxygen levels below some specific thresholds could be disruptive to marine organisms and ocean ecosystems [1]. The last Intergovernmental Panel on Climate Change (IPCC) assessment reports that 'oxygen concentrations have decreased in the open ocean thermocline in many ocean regions' since the 1960s and that 'tropical oxygen minimum zones (OMZs) have likely expanded in recent decades' [2]. The invoked mechanisms at play are a reduction of oxygen solubility due to ocean warming and the combination of reduced ventilation/increased stratification that prevents the penetration of oxygen into the interior of the ocean. Both of these mechanisms are very consistent with the global warming trend, suggesting that deoxygenation will continue with future anthropogenic climate change and would pose a risk to marine ecosystems, in addition to threats associated with ocean acidification, sea-water warming and a reduction in primary productivity [3–6].

Global Earth System models (ESMs) have been instrumental in highlighting ocean deoxygenation as a potential future threat to marine ecosystems. Back in 1998, Sarmiento and co-authors [7] simulated the response of ocean biogeochemistry to global warming using a coupled climate–marine biogeochemistry model and showed that oxygen levels in the twenty-first century could decrease by $-8\,\mathrm{mmol\,m^{-3}}$ globally, and by up to $-50\,\mathrm{mmol\,m^{-3}}$ locally. Other modelling studies have followed and confirmed these first simulated trends [8–10], including the most recent generation of ESMs used for the last assessment report of the IPCC [11,12]. These recent models suggest that the deoxygenation trend over the twenty-first century will continue irrespective of the future scenario, with an expected decrease in global ocean $O_2$ content at the end of the twenty-first century between $-1.81\%$ for the 'optimistic mitigation' scenario (RCP2.6) and $-3.45\%$ for the high-emission 'business as usual' scenario (RCP8.5) [3].

Even if current models agree well on the trend of future global deoxygenation, this is not the case at the regional level in the tropical ocean. There is as yet no consensus on the evolution of subsurface oxygen levels in the tropics (here defined from 200 to 600 m depth) and hence on the evolution of the volume of hypoxic and suboxic waters [3,11,13]. Indeed, whereas current observations show that tropical OMZs have probably expanded worldwide over the past 60 years [2,14], ESMs simulate increasing oxygen levels in the subsurface tropical Atlantic Ocean and Indian Ocean and disparate changes (increase or decrease depending on the model) in the tropical Pacific Ocean [3]. Cabré *et al.* [15] focused on the inter-model discrepancies in the Equatorial Pacific and showed that they always hide an almost perfect compensation between the warming-induced decrease in $O_2$ (i.e. saturation or thermal component) and the increase in $O_2$ associated with changes in biological productivity and ocean ventilation (i.e. the apparent oxygen utilization (AOU) or non-thermal component). Also focusing on the OMZ in the Eastern Equatorial Pacific, Ito & Deutsch [16] pointed out that the natural variability associated with the El Niño–Southern Oscillation also led to a weak response in subsurface $O_2$ levels, also resulting from the compensation between changes in $O_2$ saturation and AOU.

Another way to gain some insights into future ocean deoxygenation is to turn to past climates. Jaccard & Galbraith [17] have compiled marine sediment proxy records over the last deglaciation and have shown some remarkably coherent signals, i.e. clear oxygenation of the deep ocean but deoxygenation of the upper 1500 m of the ocean throughout the deglaciation. As for future projections, these changes illustrate the potential role of ocean ventilation and marine ecosystem changes in driving $O_2$ changes. Indeed, a simple solubility control of oxygen levels in the ocean

would not explain the contrasted changes between the upper and deeper oceans. Jaccard & Galbraith [17] hypothesized that the trend in subsurface oxygen levels (i.e. deoxygenation through deglaciation) may have been caused by an increase in carbon export from the surface layers that would have increased oxygen consumption in the subsurface ocean.

The approach we follow in this study is directly inspired from the proposal of Jaccard *et al.* [18], that is, to confront future projections of ocean deoxygenation with past geological changes, as a way to gain a perspective on how ocean oxygenation responds to large-scale climate change and variability. To do so, we build upon the work of Bopp *et al.* [3] and Cabré *et al.* [15] and analyse future projections of ocean deoxygenation, but we contrast them with past changes of ocean oxygenation from the Last Glacial Maximum (LGM) 21 000 years ago. We focus here mostly on ocean oxygenation in the subsurface waters of the tropical ocean, where ESMs do not project consistent future trends, and we compare these trends with trends at the surface and in the deep ocean. We first make use of the ESMs from the Coupled Model Intercomparison Project phase 5 (CMIP5) ensemble used by Bopp *et al.* [3], and apply a decomposition of the $O_2$ change signal into its saturation ($O_{2sat}$) and AOU components,

$$\Delta O_2 = \Delta O_{2sat} - \Delta AOU. \tag{1.1}$$

We apply this framework to future trends under the high-emission Representation Concentration Pathway 8.5 (RCP8.5) and contrast them with changes expected from natural variability exploiting multi-century-long pre-industrial climate simulations (§3). We then examine oxygen changes and their $O_{2sat}$/AOU decomposition during past climates using an LGM simulation realized with one of the above-mentioned CMIP5 models (IPSL-CM5A-LR) and data-based reconstructions of past oxygenation (§4). Finally, we give some perspectives on how future oxygenation changes can be interpreted in a larger time-scale context, by contrasting future and deglacial (de)oxygenation signals (§5).

## 2. Material and methods

### (a) CMIP5 models and simulations

We use simulations from nine ESMs from the CMIP5. The selection of models is based on the same subset as the one used in Bopp *et al.* [3] (see table 1 in Bopp *et al.* [3]). We make use of historical simulations for the period 1990–1999 (referred to as the present state) and of RCP8.5 simulations for the period 2090–2099 (referred to as the future state). To compute changes in dissolved $O_2$, as well as changes in $O_{2sat}$ and AOU, we use ocean temperature, ocean salinity and ocean dissolved oxygen concentrations as simulated by the CMIP5 models. $O_{2sat}$ is computed from temperature and salinity and AOU is deduced from $AOU = O_{2sat} - O_2$. To gain some insight into potential changes in ventilation, we use ideal ventilation age as simulated by some of the CMIP5 models. The ideal age is an 'artificial' tracer frequently used in Ocean General Circulation models to estimate simulated ventilation times. It is permanently set to zero at the surface of the ocean and increases by 1 per unit time.

We quantify oxygenation changes due to short-term natural variability using the pre-industrial control experiments called piControl performed with the same nine CMIP5 ESMs. Pre-industrial experiments diagnose the Earth System internal variability at interannual to multi-decadal time scales in the absence of anthropogenic (fossil fuel emissions, etc.) or external (volcanoes, etc.) forcing. Here, we considered the last 500 years of these pre-industrial experiments except for NorESM1-ME, which only provides 256 years.

All model outputs (RCP8.5 and piControl) have been regridded on a common $1^\circ \times 1^\circ$ grid and to standard ocean depths using a Gaussian-weighted average. A robustness index for oxygen future trends is defined when at least 80% of models agree on the sign of the mean change (robustness index larger than 1), again similar to Bopp *et al.* [3].

## (b) Palaeoclimate simulations

In addition to the control, historical and future projection simulations, we also use palaeoclimate simulations performed with the IPSL-CM5A-LR ESM [19] with the same model version as the one used for the entire CMIP5 exercise. These simulations for the periods of the mid-Holocene (MH; *ca* 6000 years ago) and the LGM (*ca* 21 000 years ago) were performed according to the CMIP5/PMIP3 protocol ([20]; http://pmip3.lsce.ipsl.fr).

The main forcing for the MH simulation is an insolation change resulting from modifications in astronomical parameters that favour an enhanced seasonal cycle in the Northern Hemisphere. The MH simulation used here is described in detail in Kageyama *et al.* [21] and we use the last 100 years of this 1000 year simulation.

The main forcings for the LGM simulation are lowered greenhouse gas concentrations and imposed LGM ice sheets. The LGM ice sheets have an impact on the land–sea distribution, topography and continental surface type. Astronomical parameters are also set to their appropriate values but this is not a very strong change compared with the present-day ones. The resulting simulation (described in Kageyama *et al.* [21] and distributed as part of CMIP5/PMIP3), which has been run for 1100 years starting from pre-industrial conditions, simulates a very strong Atlantic Meridional Overturning Circulation (AMOC), with North Atlantic Deep Waters reaching the bottom of the North Atlantic ocean. This is not very realistic compared with the current understanding of the North Atlantic circulation that emerges from a portfolio of palaeodata [22], even if the intensity of the glacial AMOC is still debated [23]. We have, therefore, (i) continued this simulation, which still displays a very strong AMOC, on the new supercomputer at our disposal and (ii) perturbed this strong AMOC simulation with a 0.2 Sv fresh-water flux imposed in the North Atlantic between 50°N and 70°N, which could be seen as an additional forcing mimicking calving fluxes from the large Northern Hemisphere ice sheets. After 200 years of hosing, the AMOC is less intense (at 6 Sv), with a boundary between the clockwise Glacial North Atlantic circulation and anti-clockwise Antarctic Bottom Waters located at around 1500 m depth in the whole Atlantic Ocean. It is this perturbed simulation which is studied here. Because this LGM simulation has not been described in detail elsewhere, we provide here in the electronic supplementary material a few additional diagnostics, showing Atlantic zonal stream functions for the LGM and the MH (electronic supplementary material, figure S4), the temporal evolution of the AMOC over the course of the LGM simulation (electronic supplementary material, figure S5) and some model-data comparison plots (electronic supplementary material, figures S6 and S7) using proxy-based reconstructions of sea-surface temperature [24], surface air temperature [25], and deep-sea temperatures and salinities [26]. Overall, the LGM simulation performs well when compared with surface reconstructions (sea-surface temperature, surface air temperature; electronic supplementary material, figure S6, and [27] for CMIP5/PMIP3 models), but, as for most of the CMIP5/PMIP3 LGM simulations, it fails to reproduce the cold and salty waters suggested by the reconstructions in the glacial Atlantic Ocean (electronic supplementary material, figure S7).

Here, we use the last 50 years of this LGM 450 year simulation (electronic supplementary material, figure S5) to depict the LGM state, and we contrast this LGM state with the MH one using the MH simulation described above. All changes shown and discussed below are computed from the LGM to the MH.

## (c) Palaeoclimate data

To gauge our palaeoclimate simulations in terms of ocean oxygenation changes, we make use of the recent multi-proxy compilation of Jaccard & Galbraith [17], reconstructing the past oxygenation state of the ocean over the last deglaciation. Reconstruction of past oxygenation is based on the analysis of sedimentary proxies of benthic oxygen levels. These proxies record modifications of the redox state at the sediment interface and are based on the presence/absence of laminations, on the assemblages of benthic foraminifera species and on redox-sensitive trace metals such as manganese and uranium. Because all these proxies have their shortcomings and

are sensitive to different $O_2$ levels, Jaccard & Galbraith [17] have included all three types to infer a relatively robust but only qualitative estimate of past changes in ocean oxygenation. Overall, the variations in past ocean (de)oxygenation have been analysed from this multi-proxy compilation for three distinct time intervals, i.e. from the LGM to Heinrich Stadial 1 (HS1), from HS1 to the Bølling–Allerød/Antarctic Cold Reversal (BA/ACR) and from the BA/ACR to the MH [17]. Because of the palaeoclimate simulations available, we focus here exclusively on the entire deglaciation period, i.e. from the LGM to the MH. For this time interval, the multi-proxy compilation includes of the order of 70 proxy records of ocean oxygenation (changes from the LGM to the MH). Note that the compilation is biased towards the Indian Basin and Pacific Basin and towards continental margins [18].

## 3. Future warming-induced (de)oxygenation

In response to the RCP8.5 forcing, the ensemble of nine ESMs analysed here simulates a robust deoxygenation trend for the surface and deep oceans (electronic supplementary material, figure S1a and d). At the surface (0–50 m average), the multi-model mean $O_2$ concentration decreases by 10 mmol $m^{-3}$ globally in the 2090s compared with the 1990s, with the largest changes occurring in the North Pacific and in the Arctic Seas (down to $-25$ mmol $m^{-3}$). In the deep ocean (2000–5000 m), the multi-model mean $O_2$ concentration decreases by 5 mmol $m^{-3}$ globally, with the largest simulated changes in the deep North Atlantic and in the deep Weddell Sea.

A focus on the subsurface ocean (200–600 m), however, reveals contrasted changes during the twenty-first century between the mid-/high latitudes, where oxygen levels drop by more than 10 mmol $m^{-3}$, and the tropics, where they increase by 5 mmol $m^{-3}$ in the Indian and Atlantic basins and stay more or less constant in the Pacific Basin (figure 1*a*). The trends at high- and mid-latitudes are consistent across the ensemble of CMIP5 models used here, but this is not the case in the tropics, especially in the Equatorial Pacific where $O_2$ changes are inconsistent across models (figure 1*a*). On average over the subsurface tropical ocean (here defined as 20°S to 20°N, 200–600 m), the multi-model mean $O_2$ concentration decreases by $-0.8$ mmol $m^{-3}$ in the 2090s (compared with the 1990s), with an inter-model standard deviation of 2.7 mmol $m^{-3}$ highlighting very large inter-model discrepancies.

### (a) Compensation between thermal and non-thermal subsurface $O_2$ changes

At the surface, simulated $O_2$ changes are controlled by changes in $O_{2sat}$ (electronic supplementary material, figure S1.b) associated with changes in sea-surface temperature and to a much lesser extent by changes in sea-surface salinity. At the surface $O_2$ concentrations remain within a few per cent of their saturation values for most of the ocean. In the deep ocean, however, simulated $O_2$ changes are controlled by changes in AOU (electronic supplementary material, figure S1.f), with only a weak contribution from decreasing $O_{2sat}$ (electronic supplementary material, figure S1.e). The increasing AOU trend, which controls the deep deoxygenation signal, is a signature of the reduction in the formation and ventilation of deep and bottom water masses formed in the North Atlantic and the Southern Ocean [28].

When focusing on the subsurface ocean (200–600 m), changes both in $O_{2sat}$ (figure 1*b*) and in AOU (figure 1*c*) play a significant role in controlling changes in $O_2$. Reductions in $O_{2sat}$ are very robust across the model ensemble and are quite homogeneous across the world ocean with the largest changes occurring where the warming is more prominent, i.e. in the Northwest Atlantic between 40°S and 50°S and in the Southern Ocean at mid-latitudes. Changes in AOU vary spatially, with increasing AOU trends at mid-latitudes (inducing reduced $O_2$ concentrations) and decreasing AOU trends at low latitudes and in the Arctic (inducing increased $O_2$ concentrations).

At mid- and high latitudes, $O_{2sat}$ and AOU reinforce each other, as expected from increasing sea-surface temperature (decreasing solubility) and reduced ventilation/increasing stratification. In the tropics, however, the $O_{2sat}$ and AOU components compensate each other so that the resulting $O_2$ change is relatively small compared with the individual components (figure 1),

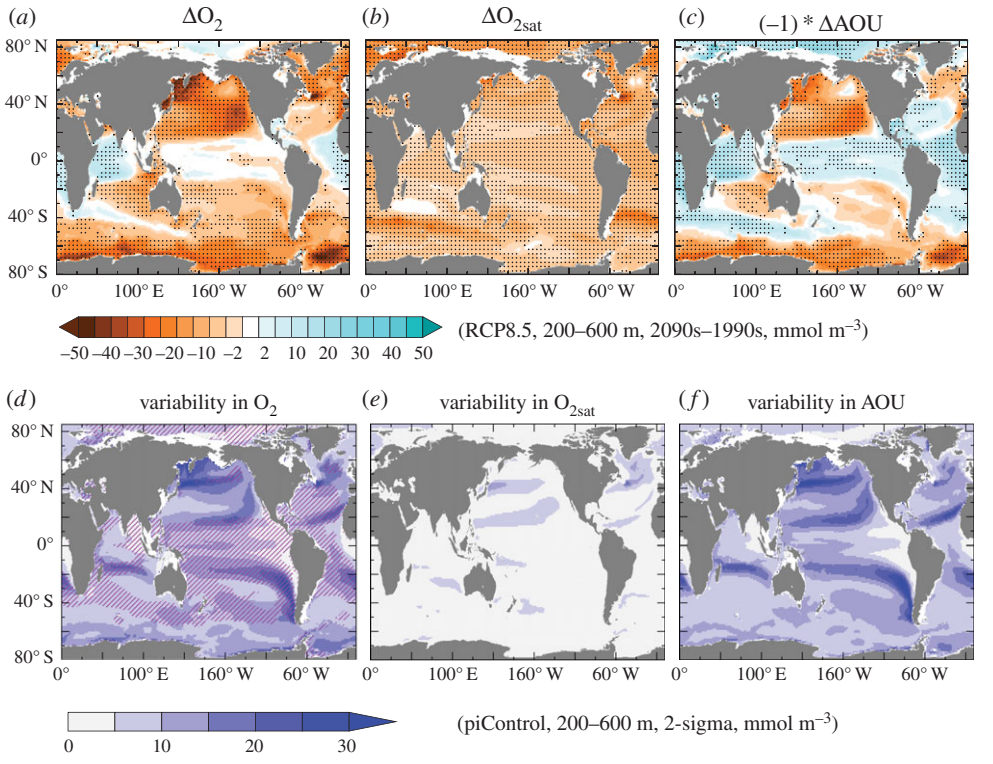


**Figure 1.** Multi-model mean changes in (*a*) subsurface dissolved $O_2$ concentrations, (*b*) subsurface $O_{2sat}$ and (*c*) subsurface AOU in 2090–2099 relative to 1990–1999 under RCP8.5 (all averaged between 200 and 600 m, in mmol $m^{-3}$). Stippling marks high robustness between models and is defined from agreement on sign of changes (i.e. when at least 80% of models agree on the sign of change). Short-term natural variability in (*d*) subsurface dissolved $O_2$ concentrations, (*e*) subsurface $O_{2sat}$ and (*f*) subsurface AOU (defined as two times the multi-model mean standard deviation computed from long pre-industrial control simulations, averaged between 200 and 600 m, in mmol $m^{-3}$). Hatching (on panel *d*) marks low detectability of future trends and is defined when the multi-model change is less than 2 s.d. of internal variability.

as shown by Cabré *et al.* [15] for the Eastern Equatorial Pacific. Although both $O_{2sat}$ and AOU changes are robust across models (when based on sign agreement between models, figure 1*b*,*c*), the magnitude of their compensation and the resulting changes in $O_2$ in the subsurface tropical ocean are not robust (figure 1*a*).

## (b) Short-term variability

$O_2$ variations associated with short-term variability (defined as two times the standard deviation) range between 0 mmol $m^{-3}$ in the core of OMZs and more than 30 mmol $m^{-3}$ in mid-latitude hot spots in the Northwest Pacific (figure 1*d*). As for future trends, we find that AOU variations largely explain the pattern of $O_2$ natural variability at the subsurface and that $O_{2sat}$ variations partly compensate the AOU signal in the tropics [15,29] but re-inforce it at mid- and high latitudes (figure 1*d*–*f*; electronic supplementary material, figure S2).

The magnitude of natural short-term variability of oxygen levels in the subsurface ocean has been a focus for some recent modelling studies in which the authors have explored the time of emergence (or detectability) of subsurface $O_2$ trends [30–32]. We find that the warming-induced change expected by the end of the twenty-first century exceeds the magnitude of natural short-term variability (at the two-sigma level) in most of the subsurface ocean at mid- and high latitudes (figure 1*d*). By contrast, we find that $O_2$ natural variations surpass the projected trends in tropical OMZs where warming-induced trends are weak due to the AOU/$O_{2sat}$ compensation

(figure 1*b*– *d*) and in regions of strong $O_2$ spatial gradients sensitive to AOU changes on shorter time scales, i.e. at the edge of OMZs and along ventilation pathways by mode and intermediate waters at mid-latitudes and by deep waters at high latitudes (figure 1*d*–*f*). The question of the emergence of a climate-driven (de)oxygenation signal is still largely debated in the literature, with a recent study by Frölicher *et al.* [4] showing that only a small fraction of the ocean area (i.e. 23%) may emerge from the noise by the end of the century under the RCP8.5 scenario.

## (c) Ventilation controls non-thermal future changes

The spatial distribution of non-thermal or AOU changes explains the spatial distribution of the $O_2$ response to climate change at the subsurface (figure 1). Here we examine the biological and physical factors controlling AOU. A reduction in biological export production would drive a decrease in AOU through reduced biological $O_2$ consumption (or oxygen utilization rates (OURs)) at depth. In parallel, an increase in ventilation or a decrease in ocean stratification would also reduce AOU without invoking any change in biological export.

At first sight, the simulated reduction in export production, which is quite prominent in the tropics for most model projections [3,33], could be thought to be responsible for the decrease in AOU (figure 2*a*). However, we find no inter-model relationship between export changes and AOU over the tropical subsurface ocean (20° S to 20° N, 200–600 m; figure 2*b*). Some models with very little change in export production project a large decrease in AOU (e.g. Geophysical Fluid Dynamics Laboratory (GFDL) models), whereas some models with a large reduction in export production only produce a small change in AOU (e.g. HadGEM2-ES). Changes in AOU are, therefore, likely to be explained by changes in ventilation, i.e. changes in $O_2$ transport by the ocean circulation and mixing.

A detailed and quantitative analysis of all $O_2$ transport terms and their changes is not possible due to the lack of these diagnostics in the CMIP5 model output. However, we can explore the relationship between changes in ventilation and changes in AOU for the models providing ocean ventilation ages. This is the case for the GFDL models. Figure 2*c*,*d* shows the changes in AOU and in an ideal age tracer in the subsurface ocean, as simulated with GFDL-ESM2G in the 2090s compared with the 1990s. These two fields show a very high spatial correlation, with a Pearson's correlation coefficient $R$ of 0.89 ($p < 0.0001$), indicating a tight control of AOU by ventilation changes. In the tropics, subsurface ventilation ages are reduced by an average of 34 years (from an average age of 382 years in the 1990s to 348 years in the 2090s), illustrating the substantial increase in subsurface ventilation with anthropogenic climate change. Although we do not have access to ventilation ages for the other CMIP5 models, the absence of a clear relationship between changes in export and changes in AOU (figure 2*b*) suggests that the increase in ventilation controls AOU changes for all or most of the models analysed here.

Several warming-induced modifications of ocean mixing and circulation could be pointed out to explain these AOU changes. With a previous version of the GFDL ESM (GFDL-ESM2.1), Gnanadesikan *et al.* [34] have analysed the processes behind the drop in ventilation time (and the subsequent increase in oxygen in the subsurface tropical Pacific). They have highlighted the role of an increase in ocean ventilation along Chile and a subsequent increase in oxygen supply due to lateral diffusion at depth. Other mechanisms/processes, the effects of which on subsurface oxygen are yet not clear, may include a deepening of the Equatorial pycnocline, mostly on the Eastern side of the ocean basins [35], an acceleration of the Equatorial Under Current [36], or an acceleration of the subtropical gyres [37]. But the most elegant explanation of a general rejuvenation of subsurface waters in response to climate change has been proposed by Gnanadesikan *et al.* [38]. They combine idealized one-dimensional simulations and global coupled simulations using an ideal age tracer and explore the impact of increased stratification and decreased ventilation. They show that global climate change may lead to younger waters at intermediate depths of the tropical oceans from changes in the relative contributions of old deep waters and younger surface waters.

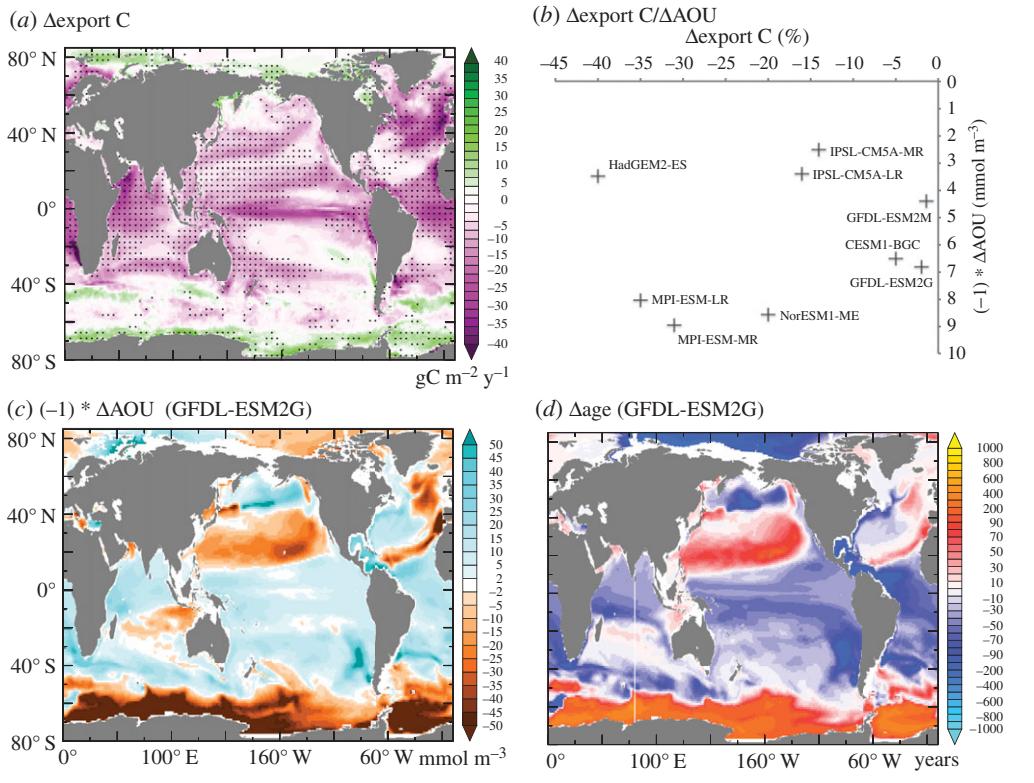


**Figure 2.** (*a*) Multi-model mean change in export production of organic particles at 100 m in 2090–2099 relative to 1990–1999 under RCP8.5. Stippling marks high robustness between models and is defined from agreement on sign of changes. (Adapted from fig. 3 of [3].) (*b*) Relation between changes in export production (from (*a*)) and changes in subsurface AOU (from figure 1*c*), averaged between 20°S and 20°N and for each of the individual ESMs used in this study. Changes as simulated by GFDL-ESM2G in (*c*) subsurface AOU (mol $m^{-3}$) and (*d*) ventilation age (years) in 2090–2099 relative to 1990–1999 under RCP8.5.

## 4. (De)oxygenation throughout the last deglaciation

Palaeoclimate records of ocean oxygenation have been used to show how oceanic oxygen levels have varied in response to past episodes of climate change. This is the case, in particular, for the last deglaciation, for which Jaccard & Galbraith [17] have revealed a clear de-oxygenation trend of the upper ocean (and hence an expansion of low-oxygen waters in the Pacific Basin and Indian Basin) concomitantly with an overall oxygenation of the deeper ocean. Despite the fact that these past changes were much slower than the current ones, they offer an interesting perspective on future ocean deoxygenation.

### (a) Model-data comparison

Due to the limited number of data points in the reconstruction we use here, we have not attempted to perform a point-by-point co-localized model-data comparison. In addition, because the simulated changes in oxygen levels between the LGM and the MH as simulated by IPSL-CM5A-LR show a certain homogeneity regardless of the longitude, we perform this comparison on a zonal average basis, as shown in figure 3.

Figure 3 shows the zonal-mean changes in oxygen concentrations in the three major ocean basins from the LGM to the MH, using the two snapshot simulations described in the Material and methods section. All ocean basins show a very striking contrast between the deep and upper oceans. The simulated deep ocean gains oxygen from the LGM to the MH, with a mean increase

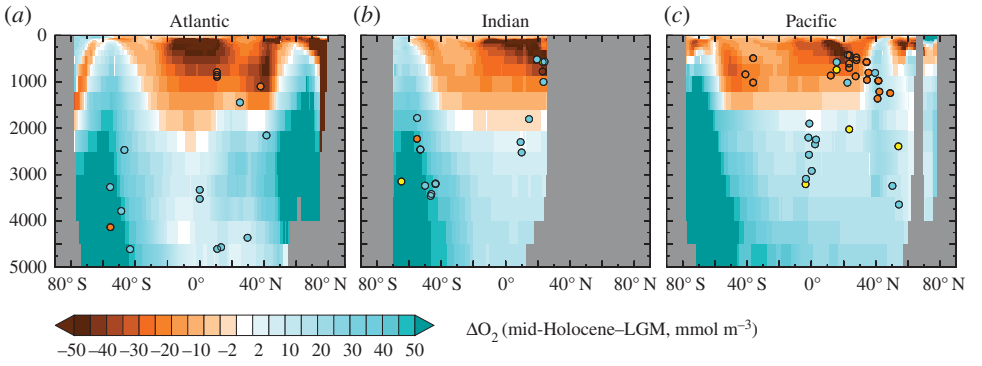


**Figure 3.** Simulated changes in dissolved oxygen (in mmol $m^{-3}$, zonal mean) from the LGM to the MH for the Atlantic Basin (*a*), Indian Basin (*b*) and Pacific Basin (*c*) (zonal mean). Plotted on top of the simulated changes are the qualitative changes in benthic oxygenation as estimated from the multi-proxy data compilation of Jaccard & Galbraith [17]. Blue (orange) indicates oxygenation (deoxygenation) from the LGM to the MH.

of 15.1 mmol $m^{-3}$ when averaged over 2000–5000 m. On the contrary, the upper ocean shows a clear deoxygenation signal with a loss of oxygen reaching 31.9 mmol $m^{-3}$ when averaged over 200–600 m and between 20° S and 20° N. Overall, the glacial ocean is simulated to be less oxygenated than at MH, with an average oxygen concentration lower by 5.8 mmol $m^{-3}$.

When the multi-proxy data compilation of Jaccard & Galbraith [17] is plotted on top of the simulated changes (figure 3), the overall comparison is rather satisfying, with the same contrast between the upper and deep oceans. If we consider the 68 records that display a significant trend (increase or decrease) from the LGM to the MH, the model reproduces the same trend for 48 of them (i.e. for 76% of the core locations). The main mismatches are located in the North Pacific, where the model simulates an oxygenation trend northward of 40°N opposite to the deoxygenation signal from the proxy records, and in the northern Indian Ocean (in fact in the Arabian Sea), where the model simulates a deoxygenation trend opposite to a clear oxygenation signal from the data. Note that all coarse resolution models have difficulties in reproducing low oxygen concentrations for the present day in these two regions (see [3] for CMIP5 models, and [39] for IPSL-CM5A-LR specifically).

## (b) Major role of ventilation changes

As for the projected trends and for the simulated short variability (§3), we decompose the $O_2$ change signal into its $\Delta O_{2sat}$ and $\Delta AOU$ components (figure 4 for the Pacific Ocean; electronic supplementary material, figure S3, for the other basins). From the LGM to the MH, $O_{2sat}$ decreases by 7.4 mmol $m^{-3}$ on average and for the global ocean, in line with a global ocean warming of 1°C. At the surface (0–50 m), the ocean warms by 2°C and $O_{2sat}$ decreases by 10.4 mmol $m^{-3}$. In the deep Southern Ocean, however, the model simulates a slight cooling of 0.1°C and a decrease in salinity of 1.1 psu, resulting in a slight increase in $O_{2sat}$.

As for the projected future trends, it is the AOU changes that drive the contrast between the upper and deep oceans (figure 4 for the Pacific Ocean; electronic supplementary material, figure S3, for the other basins). In the deep ocean (2000–5000 m), AOU decreases by 22 mmol $m^{-3}$ and drives the overall change in $O_2$ levels, being only slightly compensated by the decreasing $O_{2sat}$ signal. In the upper ocean, especially in the tropics, AOU increases along the deglaciation. In the subsurface tropical ocean (200–600 m, 20°S and 20°N), AOU increases by 21.8 mmol $m^{-3}$. The overall change in $O_2$ in the same water mass thus results from a re-inforcement of decreasing $O_{2sat}$ and increasing AOU.

As stated above, the deglacial change in AOU may be explained by changes in the sinking of organic material from the surface layers (and a corresponding change in local $O_2$ consumption),

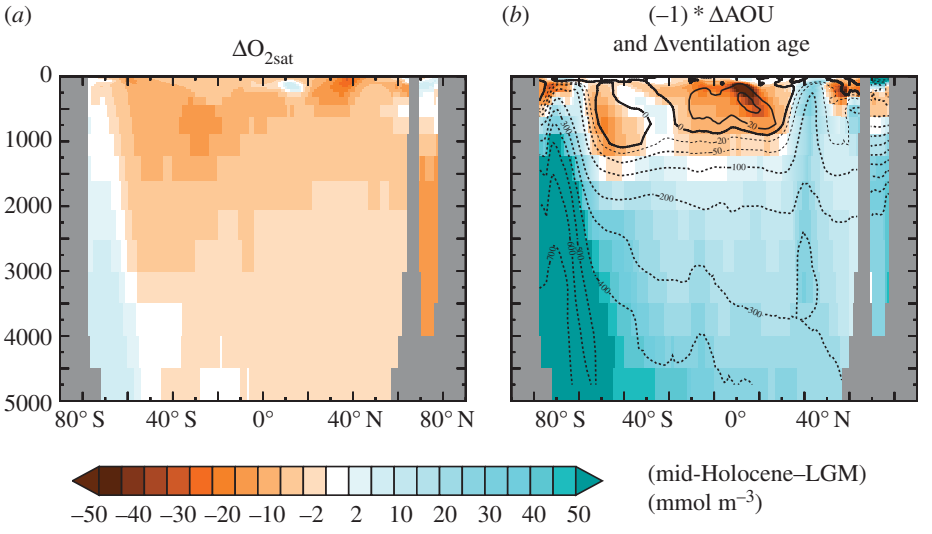


**Figure 4.** Simulated changes in (*a*) $O_{2sat}$ and (*b*) AOU (mmol m$^{-3}$) from the LGM to the MH for the Pacific Basin (zonal mean). On top of AOU changes, the contours show changes in ventilation age (years, isolines at 20, 50 and every 100 from 100 to 700 years) from the LGM to the MH.

or by some modifications of ocean ventilation. The deglacial increase in oxygen levels in the deep ocean is consistent with increased ventilation during that time interval, as shown by some circulation proxy records such as radiocarbon data [40]. But it is also consistent with a reduction of the sinking flux to the deep ocean as suggested by Jaccard & Galbraith [17]. Combining deep $O_2$ reconstructions with some proxy indicators of biological export production and of deep ventilation ages for a sediment core in the South Atlantic, Gottschalk *et al.* [41] have attributed the de-glacial oxygenation signal to a combination of physical (increased ventilation) and biological (reduced export) drivers.

The deglacial deoxygenation of the upper layers however has to be explained by a reduction in ocean ventilation for the corresponding water masses or by an increased remineralization of organic material in these depth layers. Jaccard & Galbraith [17] have discussed these different hypotheses. They show that the deglacial deoxygenation signal of the upper ocean was mostly localized in the Indo-Pacific oceans, even if it were due to increased sensitivity of sedimentary oxygenation proxies to low $O_2$ levels. They also showed that the signal was most pronounced during a rather brief time interval from the HS1 to BA/ACR transition, which was characterized by a large and abrupt warming in the Northern Hemisphere. They suggest in addition that the main driver of this intense deoxygenation could have been linked to an increase in surface production, in carbon export and in oxygen consumption at depth, caused by an increased nutrient supply associated with a shoaling and intensification of the thermocline [42].

Here, to disentangle these two combined effects (ventilation and biology), we analysed the changes in ventilation ages together with the changes in AOU. Figure 4*b* shows a very clear correspondence between AOU and ventilation changes, suggesting that AOU changes are mostly driven by these ventilation changes (see the electronic supplementary material, figure S3, for the other basins). This is in agreement with the close correspondence between the reconstructed global qualitative changes in oxygenation and proxies for deep ocean ventilation as reported by Galbraith & Jaccard [43]. In the deep Southern Ocean for instance, the decrease in AOU by more than 50 mmol m$^{-3}$ is parallel to a reduction in the ventilation age by more than 700 years. In the subsurface tropical ocean, AOU increases by up to 50 mmol m$^{-3}$ from the LGM to the MH (which is the main cause of the deoxygenation signal), whereas the simulated ventilation age increases by more than 50 years. We have not analysed in detail the dynamical changes from the LGM to the MH as simulated by IPSL-CM5A-LR, but some of the prominent features, such as (i) a

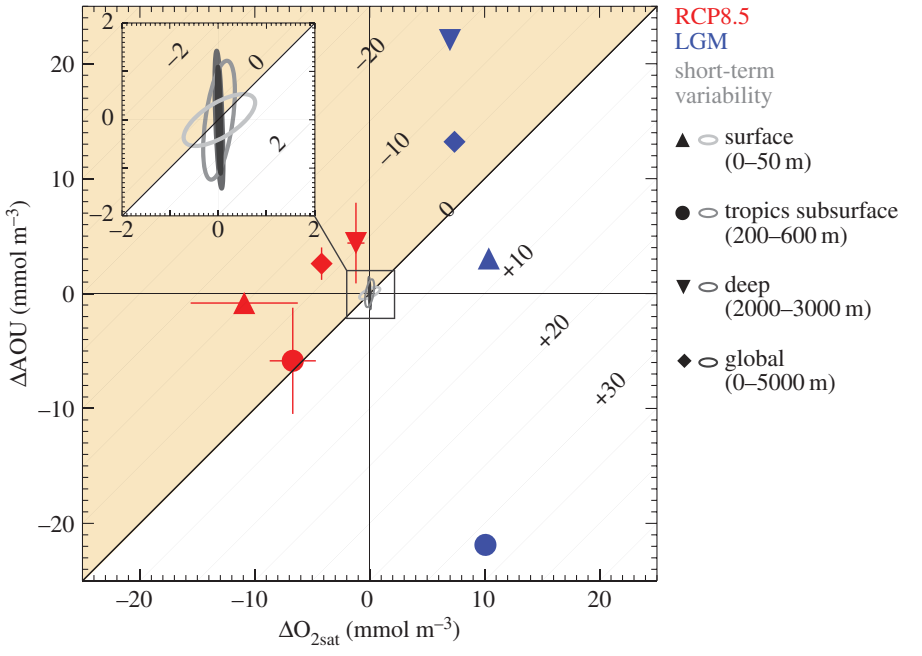


**Figure 5.** Summary figure with $O_{2sat}$ changes (*x*-axis, mmol $m^{-3}$), AOU changes (*y*-axis, mmol $m^{-3}$) and the resulting $O_2$ changes (with grey lines representing the iso-lines of total O2 changes, mmol $m^{-3}$). Diamonds are for the global ocean, triangles for the surface ocean (0–50 m, 90°S and 90°N), dots for the subsurface tropical ocean (200–600 m, 20°S and 20°N) and down triangles for the deep ocean (2000–3000 m, 90°S and 90°N). Blue depicts LGM changes relative to MH, red RCP8.5 projected changes relative to modern conditions. Grey/black ellipses show short natural term variability and are based on 95% of the internal variability of $O_{2sat}$ and AOU for the four depth levels.

re-invigoration of the AMOC from 6 to 11 Sv at the MH and (ii) an increase in Antarctic Bottom Waters (electronic supplementary material, figure S4), are clearly consistent with the changes in ventilation that we discuss above. The use of proxies of past ocean circulation, such as $^{14}C$, *PaTh* or $\varepsilon_N d$, and a direct model-data comparison using these simulated proxies, would give a much better estimate of the realism of this specific LGM past ocean circulation.

## 5. Conclusion and perspectives

Past changes do not represent *a priori* a direct constraint for future ocean (de)oxygenation. It is evident for instance that the last deglaciation has been much slower than the recent century-scale warming and that it started from a very different initial state. That said, the combined analysis of future and deglacial changes, as suggested recently by Jaccard *et al.* [18], offer some interesting insights into the use of ESMs for projecting ocean deoxygenation. They offer in particular an interesting look at the controls of the changes in dissolved oxygen in response to some climate change episodes. Figure 5 displays a combined view of $O_2$ changes across the different time periods, as simulated by the ensemble of CMIP5 models (for the projected trends and the short-term natural variability) and by the IPSL-CM5A-LR ESM (for the last deglaciation). The changes in $O_2$ are broken down into the $O_{2sat}$ and AOU components.

First, using a similar model to the one used for future projections, we show that it is indeed possible to reproduce the broad changes in oxygen concentration from the LGM to the MH, i.e. deoxygenation of the subsurface ocean/oxygenation of the deep ocean along the deglaciation. Second, we show that there is a consistent and major role of AOU and ventilation changes in driving the resulting changes in dissolved $O_2$, in the deep and the global ocean, and across the different periods considered here, that is from the LGM to future projections (figure 5). Third, we

show that compensation between AOU and $O_{2sat}$ may differ between climate periods: whereas they compensate each other for future trends in the subsurface tropical oceans, they tend to re-inforce each other at the LGM. And oppositely, whereas they re-inforce each other for future trends in the deep ocean, they tend to compensate at the LGM. Fourth, the evolution of the subsurface tropical ocean over the next decades stems from the only time scales where $O_{2sat}$ and AOU almost perfectly compensate so that changes in $O_2$ are relatively modest, making these changes harder to detect (AOU and $O_{2sat}$ reinforce each other during the last deglaciation and only partly compensate on shorter time scales, figure 5).

Several lines of work following what is presented here can be proposed. They would fill in some of the gaps and shortcomings inherent to what is exposed here.

— A more quantitative analysis of $O_2$ changes in the subsurface tropical ocean would be needed to more precisely attribute oxygen changes to potential modifications in ocean ventilation and biology. To be able to do so properly, we clearly advocate that all simulations for the next phase of CMIP now include an ideal age tracer, as well as diagnostics of all transport terms for oxygen.
— Even if clearly needed, a focus on OMZs is still difficult at this stage, because of the very large discrepancies for all models when comparing the simulated OMZs with observations [15]. This partly explains our strategy to focus on the large-scale signal of the subsurface tropical ocean. With an increase in spatial resolution in the future generation of ESMs, there is some expectation that the realism of the representation of OMZs will largely improve in the coming years [44], hence offering a better way of investigating the response of OMZs to climate change.
— Measurements of oxygen concentration over the last decades have been used to conduct model-data comparisons of the trends in $O_2$ concentrations [45–47]. The combined use of $O_2$ and of other tracers (e.g. temperature) could enable a direct estimate from the data of the contributions from the different mechanisms driving $O_2$ changes (solubility, ventilation, biology), as attempted by Helm *et al.* [48].
— It would be very interesting to pursue the kind of analysis we propose here with multi-century-scale projections [49] to see if the compensation between $O_{2sat}$ and AOU in the subsurface tropical ocean is only a transient feature.
— Last but not least, the analysis of past climate simulations and a comparison between the last deglaciation and future projections has been possible in this work thanks to one model of the CMIP5 ensemble. The combined use of past climate and future projection simulations for all models could enable some emergent constraint relationships to be derived (see [50] for a review of emergent constraint applied to cloud feedbacks) and hence potentially reduce future model uncertainties on ocean deoxygenation.

Data accessibility. All CMIP5 simulations used here can be accessed through the ESGF portal for CMIP5 at http://pcmdi9.llnl.gov. Outputs from the IPSL-CM5A-LR LGM simulation used here, which are not distributed through CMIP5, can be obtained by contacting Masa.Kageyama@lsce.ips.fr.

Authors' contributions. All authors read and approved the manuscript.

Competing interests. The author(s) declare that they have no competing interests.

Funding. EU H2020 CRESCENDO (reference no. 641816) and Labex L-IPSL (reference no. ANR-10-LABX-0018).

Acknowledgements. L.B. thanks the organizers of the Royal Society Meeting on Ocean Ventilation and Deoxygenation in a Warming World. The authors thank their national computing centres TGCC/CEA and GENCI for the attribution of computing resources and the IPSL modelling group for the software infrastructure, which facilitated CMIP5 analysis. They also acknowledge the World Climate Research Programme's Working Group on Coupled Modelling, which is responsible for CMIP. For CMIP, the US Department of Energy's Program for Climate Model Diagnosis and Intercomparison provided coordinating support and led the development of software infrastructure in partnership with the Global Organization for Earth System Science Portals. The Last Glacial Maximum simulation was run in the framework of PMIP, which is endorsed by PAGES and WCRP. P.L.M's PhD was funded by IDEX Paris-Saclay and the work on palaeoclimates by the GIWA French-Swedish project (2015–2017).

## References


1. Vaquer-Sunyer R, Duarte CM. 2008 Thresholds of hypoxia for marine biodiversity. *Proc. Natl Acad. Sci. USA* **105**, 15 452–15 457. (doi:10.1073/pnas.0803833105)
2. Rhein M *et al*. 2013 Observations: ocean. In *Climate Change 2013: The Physical Science Basis. Contribution of Working Group I to the Fifth Assessment Report of the Intergovernmental Panel on Climate Change* (eds TF Stocker *et al*.), pp. 255–310. Cambridge, UK: Cambridge University Press.
3. Bopp L *et al.* 2013 Multiple stressors of ocean ecosystems in the 21st century: projections with CMIP5 models. *Biogeosciences* **10**, 6225–6245. (doi:10.5194/bg-10-6225-2013)
4. Frölicher TL, Rodgers KB, Stock CA, Cheung WWL. 2016 Sources of uncertainties in 21st century projections of potential ocean ecosystem stressors. *Glob. Biogeochem. Cycles* **30**, 1224–1243. (doi:10.1002/2015GB005338)
5. Gruber N. 2011 Warming up, turning sour, losing breath: ocean biogeochemistry under global change. *Phil. Trans. R. Soc. A* **369**, 1980–1996. (doi:10.1098/rsta.2011.0003)
6. Pörtner H-O, Karl DM, Boyd PW, Cheung WWL, Lluch-Cota SE, Nojiri Y, Schmidt DN, Zavialov PO. 2014 Ocean systems. In *Climate Change 2014: Impacts, Adaptation, and Vulnerability. Part A: Global and Sectoral Aspects. Contribution of Working Group II to the Fifth Assessment Report of the Intergovernmental Panel on Climate Change* (eds CB Field *et al*.), pp. 411–484. Cambridge, UK: Cambridge University Press.
7. Sarmiento JL, Hughes TMC, Stouffer RJ, Manabe S. 1998 Simulated response of the ocean carbon cycle to anthropogenic climate warming. *Nature* **393**, 245–249. (doi:10.1038/30455)
8. Bopp L, Le Quéré C, Heimann M, Manning AC, Monfray P. 2002 Climate-induced oceanic oxygen fluxes: implications for the contemporary carbon budget. *Glob. Biogeochem. Cycles* **16**, 1–13. (doi:10.1029/2001GB001398)
9. Matear RJ, Hirst AC, McNeil BI. 2000 Changes in dissolved oxygen in the Southern Ocean with climate change. *Geochem. Geophys. Geosyst.* **1**, 1050. (doi:10.1029/2000GC000086)
10. Plattner G-K, Joos F, Stocker TF. 2002 Revision of the global carbon budget due to changing air-sea oxygen fluxes. *Glob. Biogeochem Cycles* **16**, 1096. (doi:10.1029/2001GB001746)
11. Ciais P *et al.* 2013 Carbon and other biogeochemical cycles. In *Climate Change 2013: The Physical Science Basis. Contribution of Working Group I to the Fifth Assessment Report of the Intergovernmental Panel on Climate Change* (eds TF Stocker *et al*.), pp. 465–570. Cambridge, UK: Cambridge University Press.
12. Stocker TF *et al*. (eds). 2013 *Climate Change 2013: The Physical Science Basis. Contribution of Working Group I to the Fifth Assessment Report of the Intergovernmental Panel on Climate Change*. Cambridge, UK: Cambridge University Press.
13. Cocco V *et al.* 2013 Oxygen and indicators of stress for marine life in multi-model global warming projections. *Biogeosciences* **10**, 1849–1868. (doi:10.5194/bg-10-1849-2013)
14. Stramma L, Johnson GC, Sprintall J, Mohrholz V. 2008 Expanding oxygen-minimum zones in the tropical oceans. *Science* **320**, 655–658. (doi:10.1126/science.1153847)
15. Cabré A, Marinov I, Bernardello R, Bianchi D. 2015 Oxygen minimum zones in the tropical Pacific across CMIP5 models: mean state differences and climate change trends. *Biogeosciences* **12**, 5429–5454. (doi:10.5194/bg-12-5429-2015)
16. Ito T, Deutsch C. 2010 Variability of the oxygen minimum zone in the tropical North Pacific during the late twentieth century. *Glob. Biogeochem. Cycles* **27**, 1119–1128. (doi:10.1002/2013GB004567)
17. Jaccard SL, Galbraith ED. 2012 Large climate-driven changes of oceanic oxygen concentrations during the last deglaciation. *Nat. Geosci.* **5**, 151–156. (doi:10.1038/ngeo1352)
18. Jaccard S, Galbraith E, Frölicher T, Gruber N. 2014 Ocean (de)oxygenation across the last deglaciation: insights for the future. *Oceanography* **27**, 26–35. (doi:10.5670/oceanog.2014.05)
19. Dufresne J-L *et al.* 2013 Climate change projections using the IPSL-CM5 Earth System Model: from CMIP3 to CMIP5. *Clim. Dyn.* **40**, 2123–2165. (doi:10.1007/s00382-012-1636-1)
20. Braconnot P, Harrison SP, Kageyama M, Bartlein PJ, Masson-Delmotte V, Abe-Ouchi A, Otto-Bliesner B, Zhao Y. 2012 Evaluation of climate models using palaeoclimatic data. *Nat. Clim. Change* **2**, 417–424. (doi:10.1038/nclimate1456)
21. Kageyama M *et al.* 2013 Mid-Holocene and Last Glacial Maximum climate simulations with the IPSL model part I: comparing IPSL-CM5A to IPSL-CM4. *Clim. Dyn.* **40**, 2447–2468. (doi:10.1007/s00382-012-1488-8)

22. Adkins JF. 2013 The role of deep ocean circulation in setting glacial climates. *Paleoceanography* **28**, 539–561. (doi:10.1002/palo.20046)
23. Lippold J *et al.* 2016 Deep water provenance and dynamics of the (de)glacial Atlantic meridional overturning circulation. *Earth Planet. Sci. Lett.* **445**, 68–78. (doi:10.1016/j.epsl.2016.04.013)
24. Waelbroeck C *et al.* 2009 Constraints on the magnitude and patterns of ocean cooling at the Last Glacial Maximum. *Nat. Geosci.* **2**, 127–132. (doi:10.1038/ngeo411)
25. Bartlein PJ *et al.* 2011 Pollen-based continental climate reconstructions at 6 and 21 ka: a global synthesis. *Clim. Dyn.* **37**, 775–802. (doi:10.1007/s00382-010-0904-1)
26. Adkins JF, McIntyre K, Schrag DP. 2002 The salinity, temperature, and $\delta^{18}O$ of the glacial deep ocean. *Science* **298**, 1769–1773. (doi:10.1126/science.1076252)
27. Masson-Delmotte V *et al.* 2013 Information from paleoclimate archives. In *Climate Change 2013: The Physical Science Basis. Contribution of Working Group I to the Fifth Assessment Report of the Intergovernmental Panel on Climate Change* (eds CB Field *et al.*), pp. 383–464. Cambridge, UK: Cambridge University Press.
28. Heuzé C, Heywood KJ, Stevens DP, Ridley JK. 2015 Changes in global ocean bottom properties and volume transports in CMIP5 models under climate change scenarios. *J. Clim.* **28**, 2917–2944. (doi:10.1175/JCLI-D-14-00381.1)
29. Ito T, Deutsch C. 2013 Variability of the oxygen minimum zone in the tropical North Pacific during the late twentieth century. *Glob. Biogeochem. Cycles* **27**, 1119–1128. (doi:10.1002/2013GB004567)
30. Frölicher TL, Joos F, Plattner G-K, Steinacher M, Doney SC. 2009 Natural variability and anthropogenic trends in oceanic oxygen in a coupled carbon cycle-climate model ensemble. *Glob. Biogeochem. Cycles* **23**, GB1003. (doi:10.1029/2008GB003316)
31. Long MC, Deutsch C, Ito T. 2016 Finding forced trends in oceanic oxygen. *Glob. Biogeochem. Cycles* **30**, 2015GB005310. (doi:10.1002/2015GB005310)
32. Rodgers KB, Lin J, Frölicher TL. 2015 Emergence of multiple ocean ecosystem drivers in a large ensemble suite with an Earth system model. *Biogeosciences* **12**, 3301–3320. (doi:10.5194/bg-12-3301-2015)
33. Laufkötter C *et al.* 2015 Drivers and uncertainties of future global marine primary production in marine ecosystem models. *Biogeosciences* **12**, 6955–6984.
34. Gnanadesikan A, Dunne JP, John J. 2012 Understanding why the volume of suboxic waters does not increase over centuries of global warming in an Earth System Model. *Biogeosciences* **9**, 1159–1172. (doi:10.5194/bg-9-1159-2012)
35. Wang G, Xie S-P, Huang RX, Chen C. 2015 Robust warming pattern of global subtropical oceans and its mechanism. *J. Clim.* **28**, 8574–8584. (doi:10.1175/JCLI-D-14-00809.1)
36. Ruggio R, Vichi M, Paparella F, Masina S. 2013 Climatic trends of the equatorial undercurrent: a backup mechanism for sustaining the equatorial Pacific production. *J. Marine Syst.* **121–122**, 11–23. (doi:10.1016/j.jmarsys.2013.04.001)
37. Cai W. 2006 Antarctic ozone depletion causes an intensification of the Southern Ocean supergyre circulation. *Geophys. Res. Lett.* **33**, L03712. (doi:10.1029/2005GL024911)
38. Gnanadesikan A, Russell JL, Fanrong Z. 2007 How does ocean ventilation change under global warming? *Ocean Sci.* **3**, 43–53. (doi:10.5194/os-3-43-2007)
39. Séférian R *et al.* 2013 Skill assessment of three Earth System models with common marine biogeochemistry. *Clim. Dyn.* **40**, 2549–2573. (doi:10.1007/s00382-012-1362-8)
40. Skinner LC, Fallon S, Waelbroeck C, Michel E, Barker S. 2010 Ventilation of the deep Southern Ocean and deglacial $CO_2$ rise. *Science* **328**, 1147–1151. (doi:10.1126/science.1183627)
41. Gottschalk J, Skinner LC, Lippold J, Vogel H, Frank N, Jaccard SL, Waelbroeck C. 2016 Biological and physical controls in the Southern Ocean on past millennial-scale atmospheric $CO_2$ changes. *Nat. Commun.* **7**, 11539 . (doi:10.1038/ncomms11539)
42. Schmittner A, Galbraith ED, Hostetler SW, Pedersen TF, Zhang R. 2007 Large fluctuations of dissolved oxygen in the Indian and Pacific Oceans during Dansgaard-Oeschger oscillations caused by variations of North Atlantic Deep Water subduction. *Paleoceanography* **22**, 3207. (doi:10.1029/2006PA001384)
43. Galbraith ED, Jaccard SL. 2015 Deglacial weakening of the oceanic soft tissue pump: global constraints from sedimentary nitrogen isotopes and oxygenation proxies. *Quat. Sci. Rev.* **109**, 38–48. (doi:10.1016/j.quascirev.2014.11.012)

44. Duteil O, Schwarzkopf FU, Böning CW, Oschlies A. 2014 Major role of the equatorial current system in setting oxygen levels in the eastern tropical Atlantic Ocean: a high-resolution model study. *Geophys. Res. Lett.* **41**, 2033–2040. (doi:10.1002/2013GL058888)
45. Ito T, Nenes A, Johnson MS, Meskhidze N, Deutsch C. 2016 Acceleration of oxygen decline in the tropical Pacific over the past decades by aerosol pollutants. *Nat. Geosci.* **9**, 443–447. (doi:10.1038/ngeo2717)
46. Stramma L, Oschlies A, Schmidtko S. 2012 Mismatch between observed and modeled trends in dissolved upper-ocean oxygen over the last 50 yr. *Biogeosciences* **9**, 4045–4057. (doi:10.5194/bg-9-4045-2012)
47. Oschlies A, Duteil O, Getzlaff J, Koeve W, Landolfi A, Schmidtko S. 2016 Patterns of deoxygenation—sensitivity to natural and anthropogenic drivers. *Phil. Trans. R. Soc. A* **375**, 20160325. (doi:10.1098/rsta.2016.0325)
48. Helm KP, Bindoff NL, Church JA. 2011 Observed decreases in oxygen content of the global ocean. *Geophys. Res. Lett.* **38**, L23602. (doi:10.1029/2011GL049513)
49. Hofmann M, Schellnhuber H-J. 2009 Oceanic acidification affects marine carbon pump and triggers extended marine oxygen holes. *Proc. Natl Acad. Sci. USA* **106**, 3017–3022. (doi:10.1073/pnas.0813384106)
50. Klein SA, Hall A. 2015 Emergent constraints for cloud feedbacks. *Curr. Clim. Change Rep.* **1**, 276. (doi:10.1007/s40641-015-0027-1)